AIP Applied Physics Letters

Mobility enhancement in amorphous InGaZnO thin-film transistors by Ar plasma treatment

Jung Han Kang, Edward Namkyu Cho, Chang Eun Kim, Min-Jung Lee, Su Jeong Lee et al.

Citation: Appl. Phys. Lett. 102, 222103 (2013); doi: 10.1063/1.4809727
View online: http://dx.doi.org/10.1063/1.4809727
View Table of Contents: http://apl.aip.org/resource/1/APPLAB/v102/i22
Published by the AIP Publishing LLC.

APPLIED PHYSICS LETTERS **102**, 222103 (2013)

Mobility enhancement in amorphous InGaZnO thin-film transistors by Ar plasma treatment

Jung Han Kang,[1] Edward Namkyu Cho,[1] Chang Eun Kim,[2] Min-Jung Lee,[3] Su Jeong Lee,[3] Jae-Min Myoung,[3] and Ilgu Yun[1,a)]

[1]*Department of Electrical and Electronic Engineering, Yonsei University, 50 Yonsei-ro, Seodaemoon-gu, Seoul 120-749, South Korea*

[2]*LG Display Co. Ltd., 1007 Deogeun-ri, Wollong-myeon, Paju-si, Gyeonggi-do 413-811, South Korea*

[3]*Department of Materials Science and Engineering, Yonsei University, 50 Yonsei-ro, Seodaemoon-gu, Seoul 120-749, South Korea*

(Received 27 April 2013; accepted 21 May 2013; published online 4 June 2013)

The effects of Ar plasma treatment on the back-channel of amorphous InGaZnO (a-IGZO) thin-film transistors are investigated. A decrease in metallic ion-oxygen bonding in the Ar plasma-treated a-IGZO channel layer was observed by X-ray photoelectron spectroscopy (XPS) depth profile analysis. An increase in the channel charge carrier concentration is estimated from the increased oxygen vacancy atomic ratio using XPS curve decomposition analysis. The plasma-treated area of the a-IGZO back-channel is varied with a photoresist screening layer with a varied open window length (L_p). From the L_p-dependent channel resistance analysis, a carrier concentration-dependent field-effect mobility enhancement is observed.
[http://dx.doi.org/10.1063/1.4809727]

Amorphous InGaZnO (a-IGZO) thin-film transistors (TFTs) have received much attention as a potential alternative material in future display applications due to its high mobility, room-temperature processibility, and large area uniformity.[1] Recently, it has been shown that improvements to stability and performance of a-IGZO TFTs can be achieved by plasma treatment on an insulator or channel layer.[2–4] In particular, mobility enhancements by plasma treatment of the source and drain channel regions have been reported as a result of a reduction in contact resistance.[3–5] However, plasma treatment of the back channel region has rarely been investigated. In this paper, channel carrier concentration-modulated performance characteristics were investigated by varying the open window length of the channel layer using a protective photo resist (PR) layer during plasma treatment.

A-IGZO TFTs were fabricated with a conventional staggered inverted bottom gate structure. A 500 nm thick SiO_2 gate dielectric was grown on a p-type silicon substrate with thermal oxidization; a 30 nm thick a-IGZO channel layer was then deposited by RF sputtering at room temperature (RT). The deposition was performed in an O_2/Ar gas flow of 5/45 sccm at a working pressure of 5×10^{-3} Torr with 150 W of RF power over 5 min. Finally, Ti source and drain electrodes were deposited with a channel overlap length (L_{ov}) of 20 μm using RF sputtering. Test structure sets were fabricated with a fixed 500 μm channel width (W) and varied channel lengths (L) ($L = 10$, 25, 50, and 100 μm) to extract the resistance components for electrical characterization of untreated and plasma-treated channel layers, respectively. To investigate the effects of plasma treatment on the channel material, open plasma treatment windows of varying lengths (L_p) were patterned using a negative PR screening layer with open lengths of $L_p = 0$, 10, 30, 50, 100, and 150 μm at the center of the surface channel. A schematic of the device structure used in our experiments is shown in Fig. 1. Plasma treatment was performed in a silica-tube by inductively coupled plasma (ICP) method for 1 min at RT with an Ar flow rate of 100 sccm, 300 W of RF power, and a working pressure of 0.4 Torr. The electrical characteristics were measured using a Keithley 236 source measurement unit (SMU). Performance parameters such as threshold voltage (V_T) and subthreshold swing (SS) were extracted by reading the gate voltage (V_G) at a drain current of $I_D = 10\,\text{nA} \times L/W$ and $SS = (dlog(I_D)/dV_G)^{-1}$, respectively. X-ray photoelectron spectroscopy (XPS) depth profiles of the plasma-treated and untreated a-IGZO active layers were obtained with Ar ion etching (ion beam: 1 kV, 1.4 μA) at a filtered Al Kα source ($h\nu = 1486.6$ eV) (Thermo VG, UK).

Fig. 2(a) shows the chemical composition of plasma-treated and untreated a-IGZO active layers with increasing etch time. Both the channel layers are estimated to have similar thicknesses by looking at the depth at which the metallic ions are reduced (In 3d, Ga 2p, and Zn 2p peaks) and the Si 2p peak rises (etch rate was approximately 0.2 nm/s). The plasma-treated channel layer shows a reduced atomic ratio of oxygen (O 1s) and increased metallic ion atomic ratios compared to the untreated channel layer. This seems due to the dissociation of oxygen atoms from metal cations under energetic Ar ion bombardment during the plasma treatment.[4] Based on this previous research, it is assumed that Ar ion with high kinetic energy penetrates and discharges into depth direction which can be estimated from the decreased O 1s throughout the plasma-treated channel layer. Thus, to investigate the depth composition of O 1s, we performed Gaussian curve fit on XPS profiles at a certain depth.

The O 1s peak is decomposed into three components with binding energies of 530.3, 531.0, and 532.3 eV (lattice oxygen, oxygen vacancies, and -OH hydroxide oxygen atoms, respectively) as shown in Figs. 2(b) and 2(c). The

[a)]Electronic mail: iyun@yonsei.ac.kr

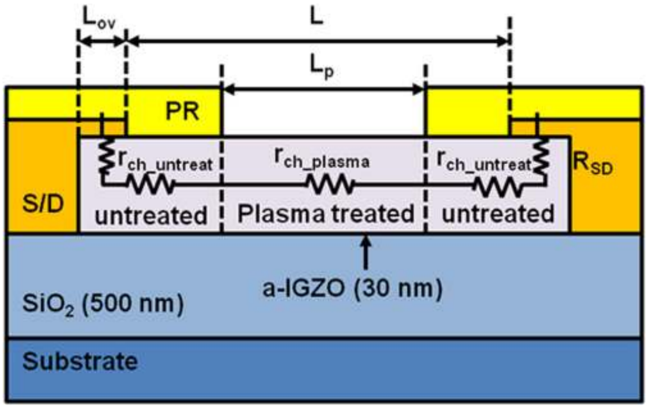

FIG. 1. Schematic diagram of a-IGZO TFT including descriptions of the electrical and structural parameters. ($W = 500\,\mu$m and $L_{ov} = 20\,\mu$m were fixed.)

decomposed curve fit of the plasma-treated channel layer's O 1s peak shows an increase in the atomic ratio of oxygen vacancies compared to that of the untreated channel layer. Due to indications in the literature that the carrier concentration is strongly correlated to oxygen deficiency, the increased oxygen vacancy atomic ratio indicates an increase in channel carrier concentration.[6–8] Oxygen vacancies increase because Ar plasma treatment disrupts metallic ion-oxygen bonding.[5,9]

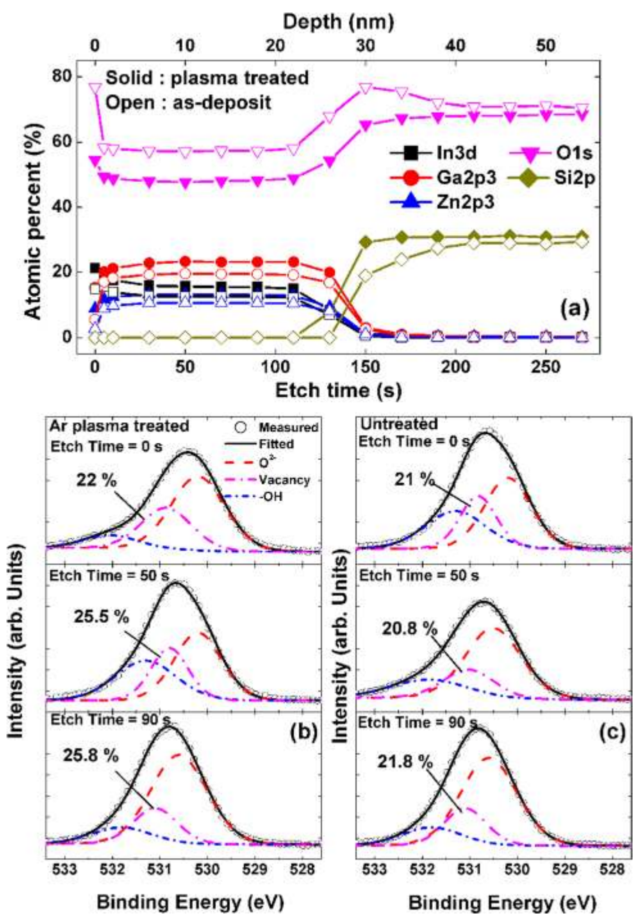

FIG. 2. (a) XPS depth profiles of an untreated (open shapes) and an Ar plasma-treated (solid shapes) a-IGZO film with increasing ion etch time. XPS curve-fits of O 1s peak of (b) treated and (c) Ar plasma untreated a-IGZO active layers with increasing etch time.

Fig. 3 shows the variation in transfer characteristics with changes in L_p. Since the plasma treatment area is proportional to L_p, the turn-on voltage (V_{ON}), which is defined as a value of V_G where I_D starts to increase sharply in the logarithmic plot of a transfer curve, shifts from -9 V to -14.5 V as L_p increases. This is due to an increase in channel carrier concentration from 1.29×10^{17} to $2.08 \times 10^{17}\,\text{cm}^{-3}$ (about 61% increase), estimated using the following equation:[10,11]

$$N_{ch} = C_i V_{ON}/q t_{ch}, \tag{1}$$

where N_{ch}, C_i, q, and t_{ch} are the channel carrier concentration, the insulator capacitance per unit area ($\sim 6.9 \times 10^{-9}$ F/cm^2), the electronic charge, and the channel thickness, respectively.

The dependence of carrier concentration on L_p was evaluated using the following equation, based on two assumptions: (1) carrier concentration is uniformly distributed in the plasma-treated and untreated regions in Fig. 1; (2) the same calculation area product of $W \times t_{ch}$ is applicable to both plasma-treated and untreated material

$$N_{ch} = \frac{N_{ch\_untreat} \times (L - L_p) + N_{ch\_plasma} \times L_p}{L}$$
$$= N_{ch\_untreat} + (N_{ch\_plasma} - N_{ch\_untreat}) \times \frac{L_p}{L}, \tag{2}$$

where N_{ch_plasma} and $N_{ch\_untreated}$ are the carrier concentrations of the plasma-treated and untreated regions, respectively. From Eq. (2), N_{ch} is linear with a positive slope with increasing L_p because $N_{ch\_untreat} = N_{ch}$ ($L_p = 0\,\mu$m) from Eqs. (1) and (2) is constant and $N_{ch\_plasma} > N_{ch\_untreat}$ from the previous XPS analysis result.

In order to verify the effects of plasma treatment on the operational properties of a-IGZO, the driving voltage (V_G-V_T)-dependent channel resistance of untreated channels ($r_{ch\_untreat}$) was extracted using the transmission line method (TLM) on an untreated test set with various L.[12] Fig. 4 (inset) shows the total resistance (R_T) response to various L_p. The plasma-treated channel resistance (r_{ch_plasma}) was extracted from the modified R_T equation as the following equations:[12]

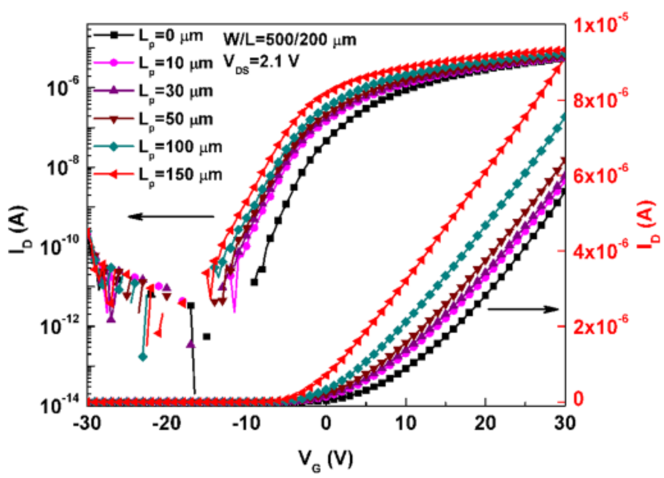

FIG. 3. Transfer characteristics of a-IGZO TFTs fabricated with varied plasma treatment window lengths (L_p). ($W/L = 500/200\,\mu$m and $V_{DS} = 2.1$ V.)

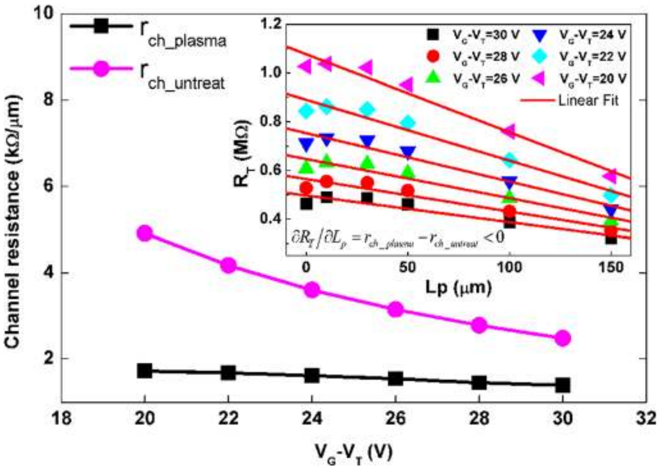

FIG. 4. Channel resistances in untreated ($r_{ch\_untreat}$) and plasma-treated (r_{ch_plasma}) regions with increasing driving-voltage (V_G-V_T). (inset) L_p dependence of total resistance (R_T) characteristics and linear-fit line for $r_{ch\_untreat}$ extraction.

$$
\begin{aligned}
R_T &= r_{ch} \times L + R_{SD} = \frac{L}{\mu_{FE} C_i W (V_G - V_T)} + R_{SD} \\
&= r_{ch\_untreat} \times (L - L_p) + r_{ch\_plasma} \times L_p + R_{SD} \\
&= r_{ch\_untreat} \times L + (r_{ch\_plasma} - r_{ch\_untreat}) \times L_p + R_{SD},
\end{aligned} \tag{3}
$$

$$
\begin{aligned}
\partial R_T/\partial L_p &= r_{ch\_plasma} - r_{ch\_untreat}; \\
r_{ch\_plasma} &= \partial R_T/\partial L_p + r_{ch\_untreat},
\end{aligned} \tag{4}
$$

$$
\partial R_T/\partial L_p = r_{ch\_plasma} - r_{ch\_untreat} < 0, \tag{5}
$$

where μ_{FE}, R_{SD}, and r_{ch} are the field-effect mobility, contact resistance, and net channel resistance, respectively.

In Eq. (3), r_{ch} was assumed to be made up of r_{ch_plasma} and $r_{ch\_untreat}$ connected in series, as shown in Fig. 1. The r_{ch_plasma} were extracted by applying Eq. (4) on inset of Fig. 4 and the previously extracted $r_{ch\_untreat}$. The extracted r_{ch_plasma} shows a reduced resistance compared to $r_{ch\_untreat}$, as shown in Fig. 4. This is due to the carrier concentration-dependent mobility characteristics indicating that the mobility increases with increasing carrier concentration and therefore the resistivity decreases.[13] The R_T decreased with increasing L_p because $r_{ch\_plasma} - r_{ch\_untreat} < 0$. Thus, the net mobility of a-IGZO TFTs increases with L_p due to reduced r_{ch}, as shown in Fig. 5 (Inset of Fig. 5 shows an example of L_p-dependent V_{ON} and μ_{FE} characteristics at V_G-$V_T = 20$ V).

In this paper, the effects of Ar plasma treatment on the back-channel of a-IGZO TFTs were investigated. Plasma-treated a-IGZO channel layer exhibited a reduction in oxygen atomic ratio from XPS depth profile. The plasma-treated open window length on the a-IGZO back-channel surface was varied using an open PR screening layer with varied L_p lengths. We have analyzed L_p dependent V_{ON} and channel resistance from the transfer characteristics. As L_p was

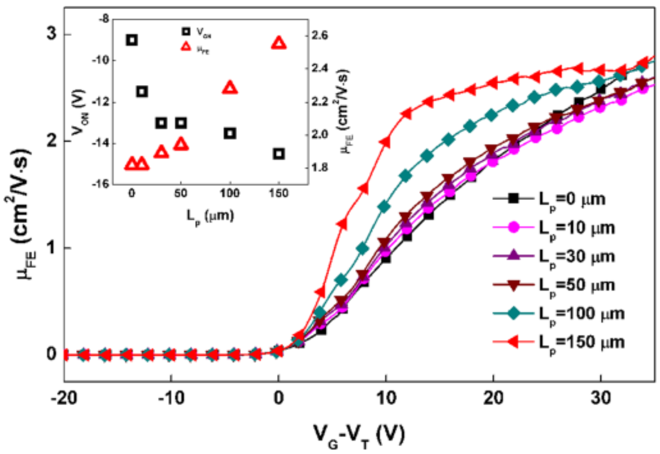

FIG. 5. Field-effect mobility (μ_{FE}) of a-IGZO TFT versus L_p. (inset) L_p dependence of V_{ON} and μ_{FE}.

increased, the V_{ON} shifted negative due to an increase in channel carrier concentration. The channel resistance showed a relationship inversely proportional with L_p. The analysis of the depth profile using curve fitting showed an increase in oxygen vacancies compared to the untreated channel layer indicating the increase of carrier concentration, which is consistent with the results of transfer characteristic. Therefore, Ar plasma treatment of the back-channel enhanced its mobility by decreasing channel resistance.

This work was supported by the WCU (World Class University) program through the National Research Foundation of Korea funded by the Ministry of Education, Science and Technology (R32-20031) and by the LG Display academic industrial cooperation program.

[1]T. Kamiya, K. Nomura, and H. Hosono, Sci. Technol. Adv. Mater. **11**, 044305 (2010).
[2]K. Remashan, D. K. Hwang, S. D. Park, J. W. Bae, G. Y. Yeom, S. J. Park, and J. H. Jang, Electrochem. Solid State Lett. **11**, H55 (2008).
[3]Y.-K. Moon, S. Lee, W.-S. Kim, B.-W. Kang, C.-O. Jeong, D.-H. Lee, and J.-W. Park, Appl. Phys. Lett. **95**, 013507 (2009).
[4]J.-S. Park, J. K. Jeong, Y.-G. Mo, H. D. Kim, and S. I. Kim, Appl. Phys. Lett. **90**, 262106 (2007).
[5]W. Kim, J.-H. Bang, H.-S. Uhm, S.-H. Lee, and J.-S. Park, Thin Solid Films **519**, 1573 (2010).
[6]T.-H. Jung, J.-S. Park, D.-H. Kim, Y. Jeong, S.-G. Park, and J.-D. Kwon, J. Vac. Sci. Technol. A **31**, 01A124 (2013).
[7]C.-T. Tsai, T.-C. Chang, S.-C. Chen, I. Lo, S.-W. Tsao, M.-C. Hung, J.-J. Chang, C.-Y. Wu, and C.-Y. Huang, Appl. Phys. Lett. **96**, 242105 (2010).
[8]K. Nomura, T. Kamiya, E. Ikenaga, H. Yanagi, K. Kobayashi, and H. Hosono, J. Appl. Phys. **109**, 073726 (2011).
[9]B. D. Ahn, H. S. Shin, H. J. Kim, J.-S. Park, and J. K. Jeong, Appl. Phys. Lett. **93**, 203506 (2008).
[10]C. E. Kim, E. N. Cho, P. Moon, G. H. Kim, D. L. Kim, H. J. Kim, and I. Yun, IEEE Electron Device Lett. **31**, 1131 (2010).
[11]N. L. Dehuff, E. S. Kettenring, D. Hong, H. Q. Chiang, J. F. Wager, R. L. Hoffman, C. H. Park, and D. A. Keszler, J. Appl. Phys. **97**, 064505 (2005).
[12]C. R. Kagan and P. Andry, *Thin-Film Transistors* (Marcel Dekker, New York, 2003).
[13]A. Takagi, K. Nomura, H. Ohta, H. Yanagi, T. Kamiya, M. Hirano, and H. Hosono, Thin Solid Films **486**, 38 (2005).